J. Chosun Natural Sci.
Vol. 10, No. 2 (2017) pp. 95 – 104
https://doi.org/10.13160/ricns.2017.10.2.95

3D-QSAR Study on Imidazopyridazines Derivatives as Potent Pim-1 Kinase Inhibitors using Region-Focused CoMFA

Pavithra K. Balasubramanian[1†], Anand Balupuri[1†], and Seung Joo Cho[1,2†]

Abstract

Proviral Integration site of Moloney (Pim) murine Leukemia virus kinases is a serine/threonine specific protein kinase. It is largely involved in cell survival and proliferation. Pim-1 phosphorylates multiple cellular substrates to inhibit apoptosis and promote cell cycle progression. Over expression of Pim-1 kinase is observed in a range of malignancies and various solid cancers. High level of Pim-1 expression is seen in myeloma, acute myeloid leukemia, prostate cancer and liver carcinomas. Hence, Pim-1 is considered as an interesting cancer target. In the present study, we have performed region-focused CoMFA study on a series of imidazopyridazine derivatives as Pim-1 kinase inhibitors. A statistically acceptable region-focused CoMFA model (q^2=0.571; ONC=3; r^2=0.909) was developed. The model was then validated using Bootsrapping and progressive sampling. The contour map highlighted the regions favorable to increase the activity. Bulky substitutions in R^2 position of the phenyl ring could increase the activity. Similarly, small negative substitution in the R^1 position of the Pyridine ring could increase the activity considerably. Our results will be useful to design novel Pim-1 kinase inhibitors of this series.

Keywords: Pim-1, Region-focused CoMFA, Imidazopyridazine Derviatives, Kinase, Inhibitors

1. Introduction

Proviral Integration site of Moloney (Pim) murine leukemia belongs to the family of serine/threonine kinases. This family of kinases is composed of three different members (Pim-1, Pim-2 and Pim-3) belonging to the $Ca2^+$/ calmodulin-dependent protein kinase group[1]. Although all 3 proteins are generally ubiquitous, there are differences in their levels of expression: Pim-1 presents higher levels in hematopoietic cells, Pim-2 in brain and lymphoid cells and PIM3 in kidney, breast and brain cells[2,3]. Pim-1 was expressed specifically in lymphoid tissue developed T-cell lymphoma[4]. Elevated levels of Pim-1 kinase were reported in human myeloid and lymphoid leukemia and lymphoma tumors[5-7], acute myeloid leukemia (AML)[8] B-cell lymphoproliferative disorders[9,10], large-cell lymphomas[11].

Departments of [1]Biomedical Sciences and [2]Cellular·Molecular Medicine, College of Medicine, Chosun University, Gwangju 501-759, Korea

[†]Corresponding author : pavithrabioinfo@gmail.com, anandbalupuri.niper@gmail.com, chosj@chosun.ac.kr
(Received : April 20, 2017, Revised : June 15, 2017, Accepted : June 25, 2017)

In addition, Pim-1 was found to be expressed in solid tumors, including pancreatic, prostate[12,13], liposarcoma[14], bladder carcinoma[15], gastric carcinoma, colorectal carcinoma, liver carcinoma, and squamous cell carcinoma[16,17]. Pim kinases are interesting targets for new drug development because of their over-expression in various cancers and involvement in cancer-specific pathways, such as cell survival, cell cycle progression and cell migration. Several inhibitors targeting PIM 1 kinases are in preclinical (SGI-1776, AR00459339) and phase 1 clinical trials (CX-4595, CXR1002). The need to design a potent and selective inhibitor for Pim-1 becomes highly important. Our group has reported several research articles on various *insilico* techniques such as application of molecular docking, and 3D-QSAR studies on kinases[18-22]. In this study, we have carried out a region-focused CoMFA study on series of imidazopyridazine derivatives.

2. Methodology

2.1. Data Set

A series of 36 imidazopyridazine derivatives were reported by Ryan *et al*., was taken for this study[23]. All

the reported IC_{50} values were converted into pIC_{50} values (-logIC_{50}). The structures of the dataset were drawn using SybylX2.1[24]. The most active compound **31** was sketched and geometry of the molecule was optimized using sybyl Tripos force field after which MMFF94 were applied as partial charge. The energy optimized conformation of compound **31**, was taken as the active conformation to draw the rest of the molecules in the dataset. The compounds taken for the study with their pIC_{50} values are tabulated (Table 1).

Table 1. Structure and Biological values of imidazopyridazines derivatives as Pim-1 kinase inhibitors

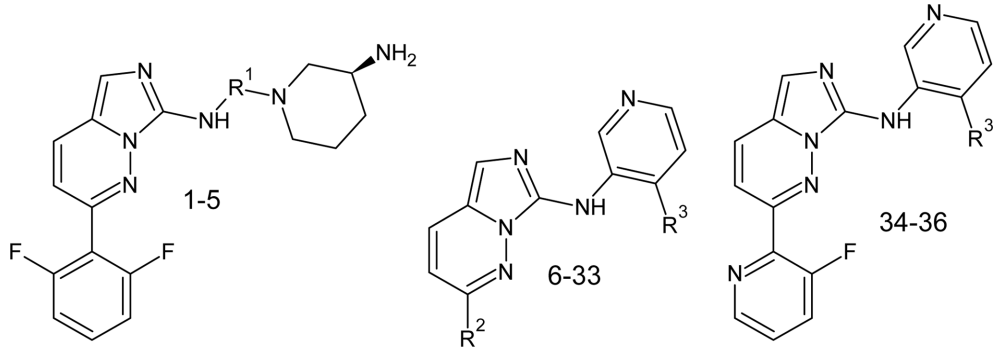

Compound	R^1	R^2	R^3	pIC_{50}
1	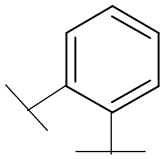	-	-	8.658
2	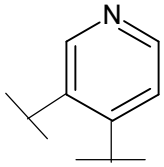	-	-	10.155
3	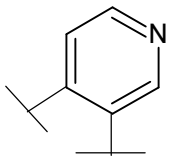	-	-	6.000
4	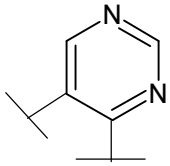	-	-	7.721
5	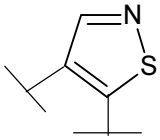	-	-	7.252

Table 1. Continued

Compound	R^1	R^2	R^3	pIC_{50}
6	-	Cl	-	7.602
7	-	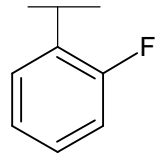	-	9.638
8	-	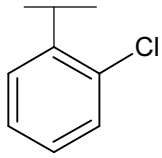	-	9.051
9	-	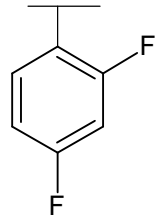	-	9.420
10	-	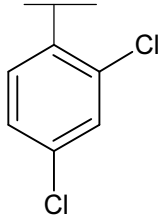	-	8.745
11	-	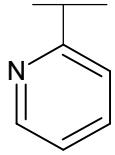	-	8.824
12	-	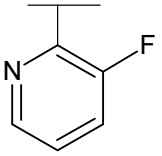	-	9.638
13	-	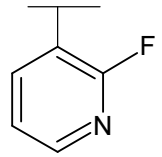	-	9.081

Table 1. Continued

Compound	R^1	R^2	R^3	pIC_{50}
14	-	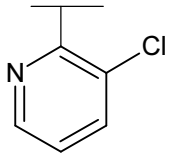	-	9.027
15	-	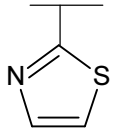	-	9.000
16	-	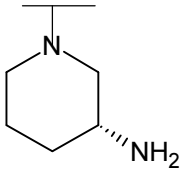	-	8.119
17	-	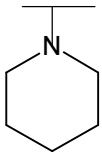	-	7.523
18	-	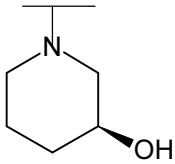	-	8.538
19	-	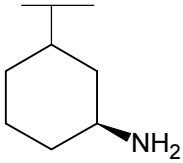	-	8.432
20	-	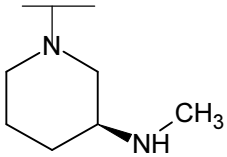	-	8.699
21	-	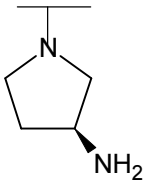	-	6.245

Table 1. Continued

Compound	R^1	R^2	R^3	pIC_{50}
22	-	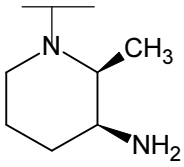	-	9.292
23	-	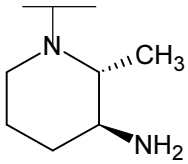	-	10.208
24	-	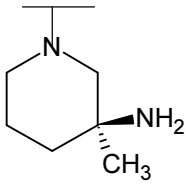	-	8.000
25	-	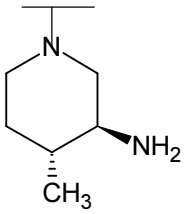	-	10.456
26	-	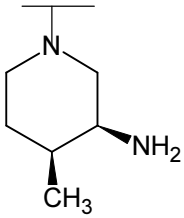	-	9.585
27	-	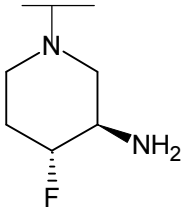	-	8.131
28	-	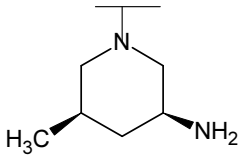	-	10.620

Table 1. Structure and Biological values of imidazopyridazines derivatives as Pim-1 kinase inhibitors

Compound	R^1	R^2	R^3	pIC_{50}
29	-	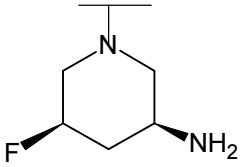	-	9.108
30	-	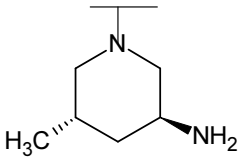	-	9.409
31	-	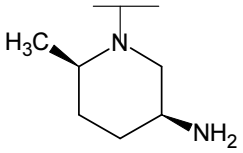	-	10.678
32	-	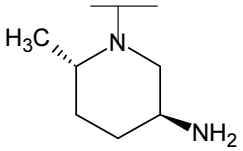	-	10.432
33	-	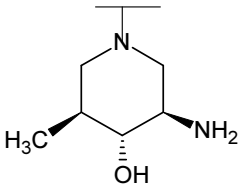	-	10.398
34	-	-	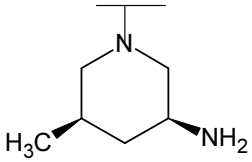	10.222
35	-	-	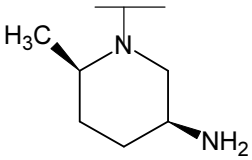	9.824
36	-	-	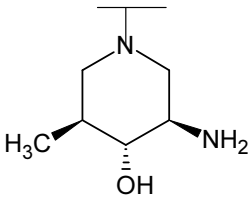	9.538

2.2. CoMFA

CoMFA was developed by Cramer *et al*[25-27]. Aligned molecules were placed in the 3D cubic lattice with the grid spacing of 2.0 Å. Steric and electrostatic fields in CoMFA were calculated from Lennard-Jones and Coulomb potentials respectively. The fields were generated using sp^3 carbon probe atom carrying +1 charge and van der Waals radius of 1.50 Å. The energy cut off of 30.0 kcal/mol was set to 30.0 kcal/mol to reduce the distortion due to extreme energy in the model.

CoMFA descriptors were used as independent variables and pIC_{50} values were used as dependent variables in the PLS analysis. A leave-one-out (LOO) was performed to determine the cross-validated r^2 (q^2). The non-cross-validated analysis was performed to determine conventional Pearson correlation coefficient (r^2) and standard error of estimate (SEE) using the ONC previously obtained from the cross-validation method.

2.2.1. Model Validation

The check the predictability and robustness of the developed model, the model was subjected validation technique such as Bootstrapping and Progressive sampling. Bootstrapping of 100 runs and progressive sampling of 100 samplings with 2 to 100 bins was performed.

3. Results and Discussion

3.1. CoMFA Model

Region-focused CoMFA model was developed for a series of imidazopyridazine derivatives. The most active compound **31** was considered as template to sketch all the compounds in the dataset. The dataset molecules were aligned using alignment method based on the common substructure. The common substructure of is shown in Fig. 1 and the alignments of the compounds are shown in Fig. 2. A reliable region-focused CoMFA model for the full dataset compounds was developed (q^2=0.571, NOC=3, r^2=0.909) with MMFF94 as partial charge. The total number of compounds in the dataset is not large. So, the data set was not divided into training and test set. Overall, the model exhibited satisfactory statistical values. The detailed statistical values for the final Region-focused CoMFA model are shown in

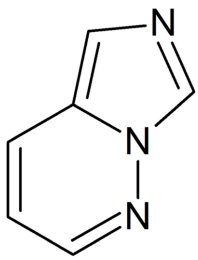

Fig. 1. Common Substructure from template compound **31**.

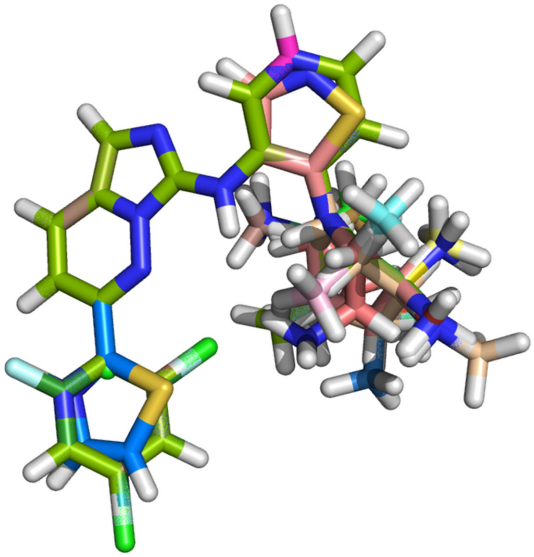

Fig. 2. Alignment of all the dataset molecules used for region-focused CoMFA.

Table 2. Statistical summary of the developed Region-Focused CoMFA model

Parameters	CoMFA MODEL
q^2	0.571
NOC	3
SEP	0.884
r^2	0.909
SEE	0.386
F value	48.017
BS r^2	0.929
BS SD	0.025
Q^2	0.532

q^2: cross-validated correlation coefficient; NOC: Number of components; SEP: Standard Error of prediction; r^2: non-validated correlation coefficient; SEE: Standard Error of Estimation; F value: F-test value; BS-r^2: Bootstrapping r^2 mean; BS-SD: Bootstrapping Standard deviation; Q^2: Progressive sampling.

Table 3. Actual and predicted pIC_{50} with their residuals of the developed Region-Focused CoMFA model

Compound	Actual pIC_{50}	CoMFA	
		Predicted	Residual
1	8.658	8.404	0.254
2	10.155	9.320	0.835
3	6.000	6.057	-0.057
4	7.721	8.285	-0.564
5	7.252	7.304	-0.052
6	7.602	7.581	0.021
7	9.638	9.262	0.376
8	9.051	9.291	-0.241
9	9.420	9.252	0.168
10	8.745	9.296	-0.552
11	8.824	8.589	0.235
12	9.638	9.042	0.596
13	9.081	9.348	-0.267
14	9.027	9.127	-0.100
15	9.000	8.986	0.014
16	8.119	7.878	0.241
17	7.523	7.949	-0.427
18	8.538	8.265	0.272
19	8.432	8.998	-0.567
20	8.699	8.295	0.404
21	6.245	6.086	0.158
22	9.292	9.552	-0.260
23	10.208	9.955	0.253
24	8.000	8.249	-0.249
25	10.456	10.541	-0.085
26	9.585	9.295	0.290
27	8.131	8.976	-0.845
28	10.620	10.394	0.226
29	9.108	9.443	-0.335
30	9.409	9.349	0.060
31	10.678	10.775	-0.097
32	10.432	9.998	0.434
33	10.398	9.885	0.513
34	10.222	10.157	0.065
35	9.824	10.432	-0.608
36	9.538	9.648	-0.111

Table 2. The experimental and predicted activity values of the molecules obtained for the ligand-based CoMFA model is tabulated in Table 3. The scatter plot and contour map for the same are shown in Fig. 3 and Fig. 4, respectively.

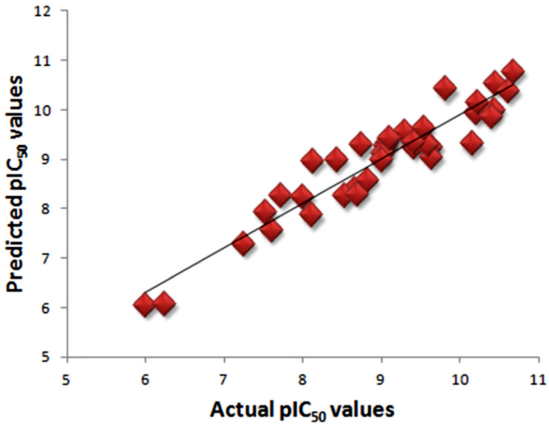

Fig. 3. Scatter plot diagram for final region-focused CoMFA model.

3.2. CoMFA Contour Maps

The contour maps were developed by using the STDEV*COEFF field. The most active compound **31** was shown superimposed inside the contour map. The steric contour map of the ligand-based CoMFA is shown in Fig. 4a. The green color and yellow color contours signify the sterically favorable and unfavorable regions respectively. A green colour contour near the NH group suggest that the bulky substitution that region could increase the activity of the compound. The two big yellow contours on either side of the piperidine ring at R^2 position suggest that bulky substitution at this position could decrease the activity. This could the reason for the decreased activity of compounds **24** and **27** which possess bulky substitution in that position.

The electrostatic contour map of the region-focused CoMFA model is shown in Fig. 4b. The blue color signifies regions favor positively charged substitution and red color signifies regions that favor negatively charged substitution. The small blue contour seen near the R^1 substitution signifies that positive substitution in that position could increase the activity. A red contour near the nitrogen atom of pyridine ring at R^1 position suggests that negative substitution favors the activity. This could validate the reason for lower activity of compounds **1** and **3** which doesn't contain negative substitution at that position. Another red color contour at R^3 position near amino group of piperidine ring suggests that negative substitution in that particular position could enhance the activity. This could validate higher

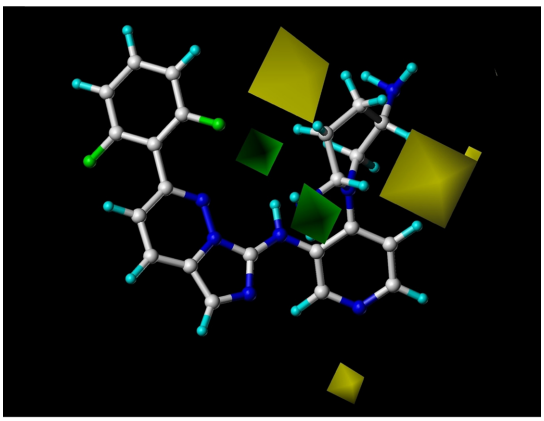

(a)

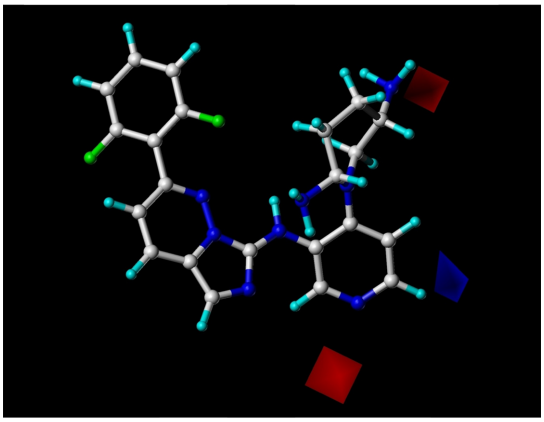

(b)

Fig. 4. (a) CoMFA Steric contour map. The green contours indicate sterically favored regions and the yellow contours denote the sterically unfavorable regions, (b) CoMFA Electrostatic contour map. The blue colored areas favor electropositive substituents and Red colored areas favors electronegative substituents.

activity of compounds **28**, **25**, **23**, **33**, **32**, and **26** including the most active compound **31** that contain negative substitution at this position possess better activity.

4. Conclusions

Pim1 kinase is an important therapeutic target due to its critical role in leukemia and various solid cancers. In the present study, we have taken a series of 36 imidazopyridazines as potent Pim1 kinase antagonist. The region-focused CoMFA model was developed with reliable statistical values. The developed model was validated using bootstrapping and progressive sampling and found to be predicable and robust. In addition, the analysis of the contour maps generated for the region-focused CoMFA model suggested the regions to increase the activity of the compounds. On the whole contour map results suggested that bulky positive substitution in R^2 position could enhance the activity. Likewise, Small negative substitution at R^1 and R^3 position could enhance the activity of the compounds. Our results provide new insights in designing novel and more potent inhibitors of imidazopyriazines series as Pim1 inhibitor.

Acknowledgements

This work was supported by the National Research Foundation of Korea grant (MRC, 2015-009070) funded by the Korea government (MSIP).

References

[1] M. C. Nawijn, A. Alendar, and A. Berns, “For better or for worse: the role of Pim oncogenes in tumorigenesis”, Nat. Rev. Cancer, Vol. 11, pp. 23-34, 2011.

[2] J. D. Feldman, L. Vician, M. Crispino, G. Tocco, M. Baudry, and H. R. Herschman, “Seizure activity induces PIM-1 expression in brain”, J. Neurosci. Res., Vol. 53, pp. 502-509, 1998.

[3] L. Brault, C. Gasser, F. Bracher, K. Huber, S. Knapp, and J. Schwaller, “PIM serine/threonine kinases in the pathogenesis and therapy of hematologic malignancies and solid cancers”, Haematologica, Vol. 95, pp. 1004-1015, 2010.

[4] T. Möröy, S. Verbeek, A. Ma, P. Achacoso, A. Berns, and F. Alt, “E mu N- and E mu L-myc cooperate with E mu pim-1 to generate lymphoid tumors at high frequency in double-transgenic mice”, Oncogene, Vol. 6, pp. 1941-1948, 1991.

[5] H. T. Cuypers, G. Selten, A. Berns, and A. H. M. Geurts van Kessel, “Assignment of the human homologue of Pim-1, a mouse gene implicated in leukemogenesis, to the pter-q12 region of chromosome 6”, Human Genetics, Vol. 72, pp. 262-265, 1986.

[6] Z. P. Wang, N. Bhattacharya, M. Weaver, K. Petersen, M. Meyer, L. Gapter, and N. S. Magnuson, “Pim- 1: a serine/threonine kinase with a role in cell survival, proliferation, differentiation and

tumorigenesis", J. Vet. Sci., Vol. 2, pp. 167-179, 2001.

[7] G. Selten, H. T. Cuypers, and A. Berns, "Proviral activation of the putative oncogene Pim-1 in MuLV induced T-cell lymphomas", EMBO J., Vol. 4, pp. 1793-1798, 1985.

[8] W. Chen, A. R. Kumar, W. A. Hudson, Q. Li, B. Wu, R. A. Staggs, E. A. Lund, T. N. Sam, and J. H. Kersey, "Malignant transformation initiated by Mll-AF9: gene dosage and critical target cells", Cancer Cell, Vol. 13, pp. 432-440, 2008.

[9] B. G. Bajaj, S. C. Verma, K. Lan, M. A. Cotter, Z. L. Woodman, and E. S. Robertson, "KSHV encoded LANA upregulates Pim-1 and is a substrate for its kinase activity", Virology, Vol. 351, pp. 18-28, 2006.

[10] E. M. Rainio, H. Ahlfors, K. L. Carter, M. Ruuska, S. Matikainen, E. Kieff, et al., "Pim kinases are upregulated during Epstein-Barr virus infection and enhance EBNA2 activity", Virology, Vol. 333, pp. 201-206, 2005.

[11] L. Pasqualucci, P. Neumeister, T. Goossens, G. Nanjangud, R. S. K. Chaganti, R. Küppers, R. Dalla-Favera, "Hypermutation of multiple proto-oncogenes in B-cell diffuse large cell lymphomas", Nature, Vol. 412, pp. 341-346, 2001.

[12] W. W. Chen, D. C. Chan, C. Donald, M. B. Lilly, and A. S. Kraft, "Pim family kinases enhance tumor growth of prostate cancer cells", Mol. Cancer Res., Vol. 3, pp. 443-451, 2005.

[13] J. Kim, M. Roh, and S. A. Abdulkadir, "Pim1 promotes human prostate cancer cell tumorigenicity and c-MYC transcriptional activity", BMC Cancer, Vol. 10, pp. 248-262, 2010.

[14] M. E. Nga, N. N. M. Swe, K. T. Chen, L. Shen, M. B. Lilly, S. P. Chan, M. Salto-Tellez, and K. Das, "PIM-1 kinase expression in adipocytic neoplasms: diagnostic and biological implications", Int. J. Exp. Pathol., Vol. 91, pp. 34-43, 2010.

[15] S. Guo, X. Mao, J. Chen, B. Huang, C. Jin, Z. Xu, and S. Qiu, "Overexpression of Pim-1 in bladder cancer", J. Exp. Clin. Cancer Res., Vol. 29, pp. 161-167, 2010.

[16] N. Shah, B. Pang, K. G. Yeoh, S. Thorn, C. S. Chen, M. B. Lilly, et al., "Potential roles for the PIM1 kinase in human cancer-a molecular and therapeutic appraisal", Eur. J. Cancer, Vol. 44, pp. 2144-2151, 2008.

[17] M. Bachmann and T. Möröy, "The serine/threonine kinase Pim-1", Int. J. Biochem. Cell Biol., Vol. 37, pp. 726-730, 2005.

[18] P. K. Balasubramanian, A. Balupuri, and S. J. Cho, "A CoMFA study of phenoxypyridine-based JNK3 inhibitors using various partial charge schemes", J. Chosun Natural Sci., Vol. 7, pp. 45-49, 2014.

[19] P. K. Balasubramanian and S. J. Cho, "HQSAR analysis on novel series of 1-(4-phenylpiperazin-1-yl-2-(1H-Pyrazol-1-yl) ethanone derivatives targeting CCR1", J. Chosun Natural Sci., Vol. 6, pp. 163-169, 2013.

[20] A. Balupuri and S. J. Cho, "Exploration of the binding mode of indole derivatives as potent HIV-1 inhibitors using molecular docking simulations", J. Chosun Natural Sci., Vol. 6, pp. 138-142, 2013.

[21] C. G. Gadhe and S. J. Cho, "Importance of silicon atom in the drug design process", J. Chosun Natural Sci., Vol. 5, pp. 229-232, 2012.

[22] S. J. Cho, "The importance of halogen bonding: A tutorial", J. Chosun Natural Sci., Vol. 5, pp. 195-197, 2012.

[23] R. P. Wurz, C. Sastri, D. C. D'Amico, B. Herberich, C. L. M. Jackson, L. H. Pettus, A. S. Tasker, B. Wu, N. Guerrero, J. R. Lipford, J. T. Winston, Y. Yang, P. Wang, Y. Nguyen, K. L. Andrews, X. Huang, M. R. Lee, C. Mohr, J. D. Zhang, D. L. Reid, Y. Xu, Y. Zhou, and H.-L. Wang, "Discovery of imidazopyridazines as potent Pim-1/2 kinase inhibitors." Bioorg. Med. Chem. Lett., Vol. 26, pp. 5580-5590, 2016.

[24] SYBYLx2.1, Tripos International, 1699 South Hanley Road, St. Louis, Missouri, 63144, USA.

[25] R. D. Cramer, D. E. Patterson, and J. D. Bunce, "Comparative molecular field analysis (CoMFA). Effect of shape on binding of steroids to carrier proteins", J. Am. Chem. Soc., Vol. 110, pp. 5959-5967, 1988.

[26] P. K. Balasubramanian, A. Balupuri, and S. J. Cho, "3D QSAR study on pyrrolopyrimidines-based derivatives as LIM2 kinase inhibitors", J. Chosun Natural Sci., Vol. 8, pp. 285-292, 2015.

[27] P. K. Balasubramanian, A. Balupuri, and S. J. Cho, "3D QSAR studies of Mks (TTK) kinase inhibitors based on CoMFA", Vol. 9, pp. 113-120, 2016.